

Correlations and flavors in jets in ALICE

Filip Krizek for the ALICE collaboration

Nuclear Physics Institute, Hlavní 130, Řež, Czech Republic

E-mail: filip.krizek@cern.ch

Abstract. We report on the measurement of hadron composition in charged jets in pp at $\sqrt{s} = 7$ TeV and show the first data on particle type dependent jet fragmentation at the LHC. Further, we present $(\Lambda + \bar{\Lambda})/2K_S^0$ ratios measured in charged jets in Pb–Pb collisions at $\sqrt{s_{NN}} = 2.76$ TeV and in p–Pb collisions at $\sqrt{s_{NN}} = 5.02$ TeV. While the ratio of the inclusive p_T spectra of Λ and K_S^0 exhibits centrality dependent enhancement both in Pb–Pb and p–Pb system, the $(\Lambda + \bar{\Lambda})/2K_S^0$ ratio measured in charged jets reveals that jet fragmentation does not contribute to the observed baryon anomaly.

Finally, we discuss the measurement of semi-inclusive p_T spectra of charged jets that recoil from a high- p_T hadron trigger in Pb–Pb and pp collisions at $\sqrt{s_{NN}} = 2.76$ TeV and $\sqrt{s} = 7$ TeV, respectively. The jet yield uncorrelated with the trigger hadron is removed at the event-ensemble level without introducing a bias on the jet population which is therefore infrared and collinear safe. The recoil jet yield in central Pb–Pb is found to be suppressed w.r.t. that from pp PYTHIA reference. On the other hand, there is no sign of intra-jet broadening even for anti- k_T jets with a resolution parameter as large as $R = 0.5$.

1. Introduction

A jet is a collimated spray of particles that is produced in the process of parton showering when a highly virtual parton fragments. Since it is ambiguous to associate final state hadrons with initial partons, the assignment of hadrons to jets is based on the decision of reconstruction algorithm. Jet reconstruction algorithms are designed to recover the four-momentum of the initial parton by summing up momenta of particles in the final state. In order to have a clear correspondence between jets in theory and experiment, jet algorithms have to be infrared and collinear safe [1].

Jets have several useful properties which predestine them as a convenient probe to study the medium created in a collision of two relativistic nuclei. First of all, we have a good understanding of jet production on perturbative QCD level in elementary reactions. Further, it is known that processes with large four-momentum transfer Q^2 occur in the initial stage of the nucleus-nucleus collision before the quark gluon plasma is formed. Hard-scattered partons then interact with the medium of deconfined quarks and gluons and loose energy. This is manifested by the so-called jet quenching phenomenon when a jet pair with a high transverse momentum imbalance is observed [2, 3]. The principal goal why the jet-medium interaction is studied is to understand the nature of medium-induced parton energy loss mechanism and its possible connection to the strongly coupled limit of QCD.

2. Jets in ALICE

A detailed description of the ALICE detector can be found in [4]. Here let us just briefly mention that precise tracking is provided by a six-layered silicon vertex tracker in combination with a large Time Projection Chamber (TPC). Both detectors are placed in the core of ALICE central barrel where the solenoidal magnetic field reaches 0.5 T. ALICE has nearly uniform acceptance and efficiency coverage for tracks in the pseudorapidity range $|\eta| < 0.9$ in the full azimuth throughout a wide transverse momentum range from ≈ 150 MeV/ c to 100 GeV/ c . ALICE has also partial coverage by the electromagnetic calorimeter EMCal which covers 107 deg in azimuth and $|\eta| < 0.7$ in pseudorapidity.

Jets are reconstructed either from tracks only (*charged jets*) or by combining tracks and calorimeter clusters (*full jets*). Whereas charged jets can be reconstructed in the full azimuth, acceptance of full jets is restricted by the incomplete coverage of the electromagnetic calorimeter. In order to remove partially reconstructed jets that appear at the boarder of the ALICE acceptance, the jet pseudorapidity range is limited by means of a fiducial cut, namely for charged jets we use $|\eta_{\text{jet}}| < 0.9 - R$, where R is the resolution parameter of the given jet algorithm. Jets are reconstructed using the infrared and collinear safe anti- k_T and k_T algorithms [5].

Soft bulk hadrons created in a heavy-ion collision constitute a significant background for jet reconstruction and cause a shift in the jet energy scale. The transverse momentum of reconstructed jets $p_{T,\text{jet}}^{\text{raw}}$ is therefore corrected for the average contribution of the bulk hadrons using the formula

$$p_{T,\text{jet}} = p_{T,\text{jet}}^{\text{raw}} - \rho A_{\text{jet}}$$

where A_{jet} denotes jet area and ρ is the mean background density. The mean background density is estimated on an event-by-event basis employing the standard area based method [6]. The finite width of the jet energy resolution is given by two sources. The first source of jet energy smearing are the local background fluctuations that occur in each event. The second contributor to the jet energy resolution are detector effects. The response matrix that relates the p_T of reconstructed and true jets is assumed to factorize into a product of matrices that describe momentum smearing by local background fluctuations and momentum smearing by detector effects. The matrix is inverted by means of common regularized unfolding techniques based on the SVD decomposition [7] or Bayes' theorem [8] implemented in the RooUnfold package [9].

3. Hadron structure of charged jets in pp collisions at $\sqrt{s} = 7$ TeV

Data on hadron composition of jets provides an important benchmark for the theory and is also needed for the fine tuning of the commonly used event generators such as PYTHIA [10]. ALICE has measured the inclusive p_T spectra of hadrons in charged jets in pp collisions at $\sqrt{s} = 7$ TeV [11]. To extract the yields of identified particles in a given track p_T bin, we use the ionization energy loss dE/dx measured by the ALICE TPC. The fractions of the most abundant particle species, which are π , K, p and e, are extracted using two methods. The first one parameterizes the dE/dx distribution corresponding to individual particle species in a given track p_T bin with Gaussian functions that have the width and mean constrained by an analytic model [12, 13]. The second approach substitutes the Gaussian functions with data driven templates of particle dE/dx [14]. Both models provide consistent results.

In Fig. 1 we present the fully corrected p_T spectra of pions, kaons and protons in charged anti- k_T jets with $R = 0.4$. This data is the first measurement of particle type dependent jet fragmentation at the LHC. Let us just briefly mention that the relative abundance of K w.r.t. π grows with the increasing fraction of p_T carried by the particle in the jet. On the other hand, with the increasing fraction of p_T carried by the jet constituent, protons are getting suppressed w.r.t. pions which signalizes the suppression of the leading baryon in the jet.

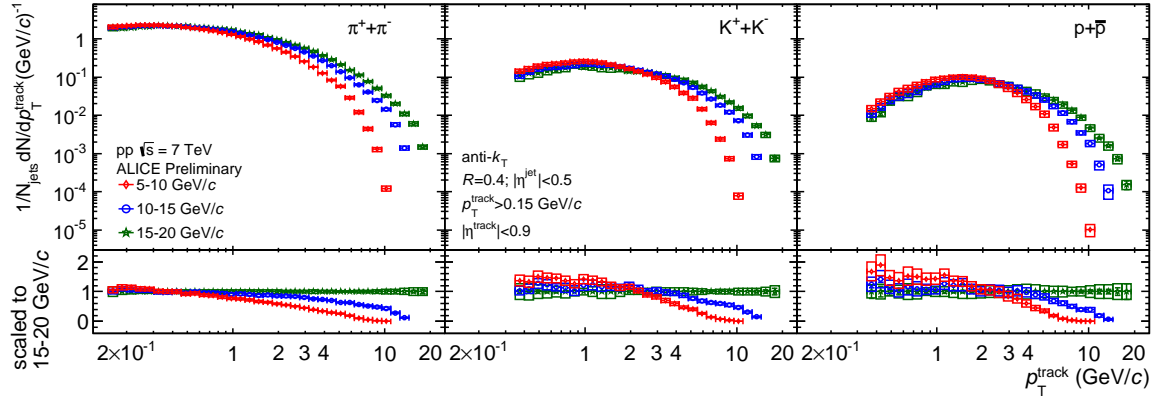


Figure 1. p_T spectra of π , K, and p in anti- k_T jets with $R = 0.4$ in pp collisions at $\sqrt{s} = 7$ TeV. The spectra are shown for three jet transverse momentum bins: 5–10 GeV/c, 10–15 GeV/c, and 15–20 GeV/c.

4. Λ/K_S^0 ratio in charged jets in Pb–Pb and p–Pb

In [15], PHENIX reported that the ratio of the inclusive p_T spectra of p to π exhibits a strong centrality dependence in Au–Au collisions at $\sqrt{s_{NN}} = 200$ GeV. A similar behavior of the ratio was observed also for other baryon to meson ratios, e.g., Λ/K_S^0 [16]. Hence, this effect is sometimes referred to as the baryon anomaly.

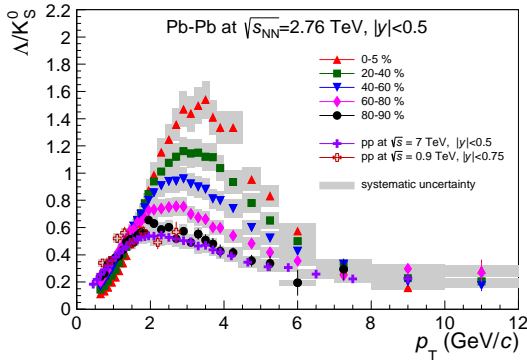


Figure 2. Ratio of inclusive p_T spectra of Λ and K_S^0 measured in Pb–Pb and pp collisions. Centrality bins used in Pb–Pb are quoted in legend. For more details see [17].

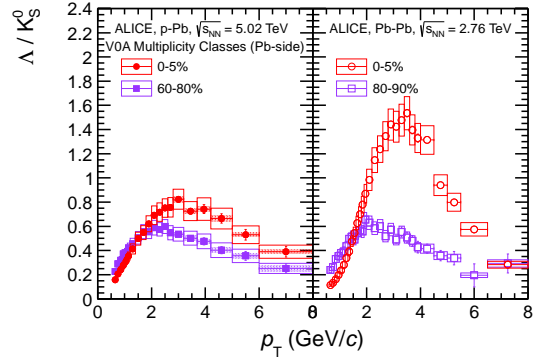


Figure 3. Ratio of inclusive p_T spectra of Λ and K_S^0 measured in p–Pb (left) and Pb–Pb (right) collisions. The corresponding centrality selections are quoted in the legend. See [25] for more details.

Using Λ and K_S^0 particles allows to extend particle identification to higher transverse momentum when compared to the p/ π case. Figure 2 shows the ratio of inclusive spectra of Λ and K_S^0 as measured by the ALICE experiment in Pb–Pb collisions at $\sqrt{s_{NN}} = 2.76$ TeV and in pp at $\sqrt{s} = 0.9$ TeV and 7 TeV [17]. While pp and peripheral Pb–Pb collisions have compatible Λ/K_S^0 ratios, in more central Pb–Pb collisions, a gradually increasing enhancement in the range 2–7 GeV/c is observed. Above 7 GeV/c, all data sets tend to pp which indicates that the dominant mechanism for particle production in this region is the jet fragmentation. On the other hand, the evolution of the ratio below 2 GeV/c with p_T and centrality is well reproduced by a hydro model calculation [17, 18, 19, 20]. The underlying mechanism of particle

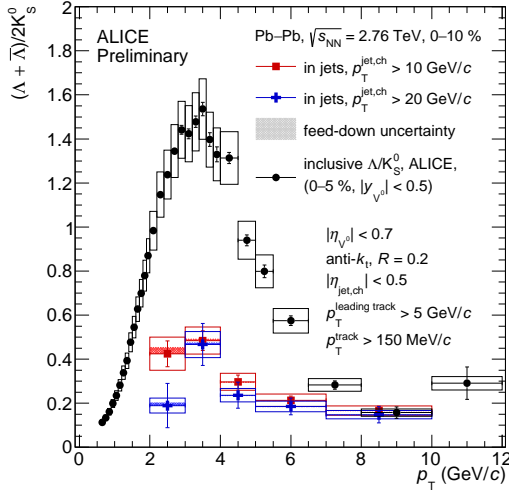


Figure 4. Ratio of p_T spectra of $\Lambda + \bar{\Lambda}$ and K_S^0 measured in 0–10% most central Pb–Pb collisions at $\sqrt{s_{NN}} = 2.76$ TeV. Black circles show the ratio obtained from inclusive spectra, red squares and blue crosses correspond to the ratios measured in charged jets with transverse momentum larger than 10 GeV/ c and 20 GeV/ c , respectively.

production in the range 2–7 GeV/ c is still a matter of discussion [21, 23, 22, 24] but note that the signature of baryon anomaly is seen also in the p–Pb at $\sqrt{s_{NN}} = 5.02$ TeV system [25], see Fig. 3. In these small systems, flow-like patterns might emerge due to the color reconnection as suggested by [26].

A natural question to be asked is whether the baryon anomaly is produced only in the bulk or whether some in-medium modified jet fragmentation also contributes. An answer to this question was searched for in the Pb–Pb and p–Pb data in parallel. The analysis required to divide V^0 candidates into two groups: i) V^0 s that can be associated with a jet and ii) V^0 that come from the underlying event. Charged jets were reconstructed using the anti- k_T algorithm with resolution parameter $R = 0.2, 0.3$ and 0.4 . In order to have in the Pb–Pb system a better separation between the combinatorial background jets that are composed of underlying event particles only and the real jets that contain particles produced by parton fragmentation, jets were required to contain a leading track with p_T larger than 5 GeV/ c . Note that such condition makes the selected sample of jets more biased as will be discussed in the next section.

V^0 reconstruction was based on charged decay channels $\Lambda \rightarrow p + \pi^-$ and $K_S^0 \rightarrow \pi^+ + \pi^-$ and employed topological cuts. As the decay daughters of V^0 particles are secondary tracks they were excluded from the jet reconstruction procedure. The decision to associate Λ or K_S^0 candidate with a given jet was done based on their mutual angular distance,

$$\sqrt{\Delta\varphi_{\text{jet}, V^0}^2 + \Delta\eta_{\text{jet}, V^0}^2} < R.$$

Here $\Delta\varphi_{\text{jet}, V^0}$ ($\Delta\eta_{\text{jet}, V^0}$) denote the azimuthal angle (pseudorapidity) distance between the V^0 candidate momentum and the jet axis and R is the jet resolution parameter. The extracted yield of V^0 candidates in jets was corrected for the expected contribution of V^0 from the underlying

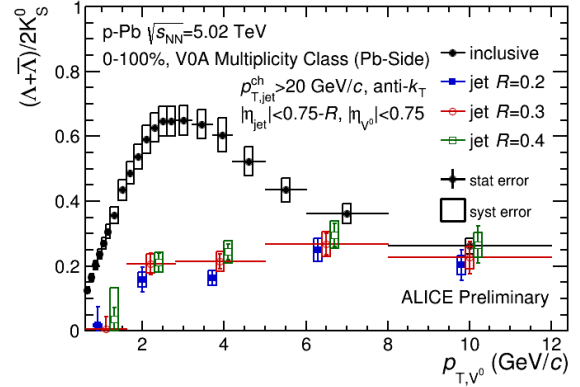


Figure 5. Ratio of p_T spectra of $\Lambda + \bar{\Lambda}$ and K_S^0 measured in minimum bias p–Pb collisions at $\sqrt{s_{NN}} = 5.02$ TeV. Black circles show the ratio obtained from inclusive spectra. Color markers show the ratio measured in charged anti- k_T jets for three sizes of the resolution parameter R . Charged jets have transverse momentum larger than 20 GeV/ c .

event and for the reconstruction efficiency. In addition, the yield of Λ particles was corrected for a contribution coming from the feed down of Ξ cascades.

Figures 4 and 5 compare the $(\Lambda + \bar{\Lambda})/2K_S^0$ ratio obtained from the inclusive V^0 s and from V^0 s associated with jets with $p_{T,\text{jet}}^{\text{ch}} > 20$ GeV/ c in central Pb–Pb collisions at $\sqrt{s_{\text{NN}}} = 2.76$ TeV and in two centrality bins of p–Pb collisions at $\sqrt{s_{\text{NN}}} = 5.02$ TeV. In both systems, the ratio measured in jets is significantly lower than the inclusive one. This observation thus supports the picture that fragmentation of hard partons producing charged jets with $p_{T,\text{jet}}^{\text{ch}} > 20$ GeV/ c does not contribute to the observed baryon anomaly. A similar conclusion was reported also earlier for p/π ratio using two particle correlations [27]. The source of the baryon anomaly thus seems to be intimately connected with partons having smaller transverse momenta [21].

5. h-jet correlation measurement

The multiplicity of hadrons in a central heavy-ion collision is large. In such an environment, the jet reconstruction algorithm often clusters together just soft bulk particles. As a result an artificial jet is created. One possibility how to suppress the number of these artificial jets is to require that the reconstructed jet contains at least one constituent with p_T above some preset threshold. This condition, however, imposes a bias on the jet fragmentation which can be unwanted especially in the situation when we look for quenched jets.

Hadron-jet coincidence measurements offer an elegant way how to overcome this problem. The approach which we will discuss allows to remove the contribution of combinatorial background jets including multi-parton interaction without imposing fragmentation bias on the reconstructed jet. The method is data driven and can be used also for jets with large R and low p_T . The detailed description can be found in [28, 29].

The basic steps of the analysis can be summarized as follows. We select events that contain a high- p_T hadron (trigger track). The presence of a high- p_T hadron identifies collisions where a hard scattering occurred. In these events, we analyze jets that recoil nearly back to back in azimuth w.r.t. to the trigger track; e.g., in this analysis, it was requested that the opening angle between the trigger track and the recoiling jet is larger than $\pi - 0.6$ rad in azimuth. Figure 6 shows a comparison of two per trigger normalized background density corrected semi-inclusive p_T distributions of recoil jets associated to exclusive trigger p_T bins, $p_{T,\text{trig}} \in \{20, 50\}$ GeV/ c and $p_{T,\text{trig}} \in \{8, 9\}$ GeV/ c . For brevity from now on $p_{T,\text{trig}}$ will be labeled as TT. In general, a trigger track with larger p_T comes on average from a hard scattering process with larger Q^2 , therefore also the corresponding recoil jet p_T spectrum is harder. Nevertheless, in the region where the mean background density corrected jet p_T is around or below zero, both spectra turn out to be nearly identical. This part of the distribution is dominated by accidental combinations of the trigger track with uncorrelated combinatorial background jets. The data suggests that the number of such combinations is largely independent of TT bin.

Assuming that the number of combinatorial background jets associated with a trigger track is independent of trigger track p_T , it is possible to introduce the following observable

$$\Delta_{\text{recoil}} = \frac{1}{N_{\text{trig}}} \frac{d^2 N_{\text{jet}}}{dp_{T,\text{jet}}^{\text{ch}} d\eta_{\text{jet}}} \Big|_{\text{TT}\{20,50\}} - \frac{1}{N_{\text{trig}}} \frac{d^2 N_{\text{jet}}}{dp_{T,\text{jet}}^{\text{ch}} d\eta_{\text{jet}}} \Big|_{\text{TT}\{8,9\}} \quad (1)$$

where N_{trig} is the number of trigger tracks in a given TT bin. In this observable the contribution of combinatorial background jets is removed. Further, let us point out that Δ_{recoil} has a direct link to theory, since the per trigger yield of recoil jets can be expressed in terms of the cross-section to produce a high- p_T hadron and the cross section to produce a high- p_T hadron together with a jet, i.e.,

$$\frac{1}{N_{\text{trig}}^{\text{AA}}} \frac{d^2 N_{\text{jet}}^{\text{AA}}}{dp_{T,\text{jet}}^{\text{ch}} d\eta_{\text{jet}}} \Big|_{p_{T,\text{trig}} \in \text{TT}} = \left(\frac{1}{\sigma^{\text{AA} \rightarrow \text{h} + \text{X}}} \cdot \frac{d^2 \sigma^{\text{AA} \rightarrow \text{h} + \text{jet} + \text{X}}}{dp_{T,\text{jet}}^{\text{ch}} d\eta_{\text{jet}}} \right) \Big|_{p_{T,\text{h}} \in \text{TT}} \quad (2)$$

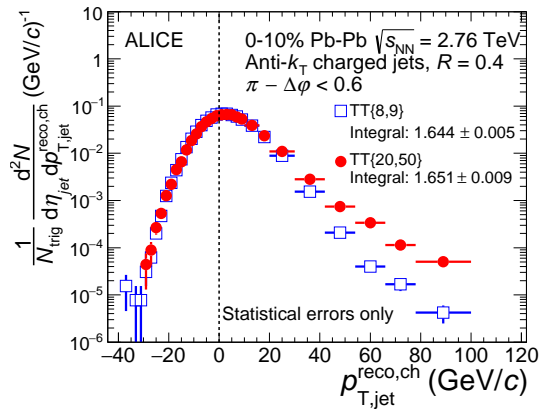


Figure 6. Semi-inclusive distributions of jets recoiling from a hadron trigger with $p_{T,\text{trig}} \in \{20, 50\}$ GeV/ c (red circles) and $p_{T,\text{trig}} \in \{8, 9\}$ GeV/ c (blue squares) for 0–10% central Pb–Pb collisions at $\sqrt{s_{\text{NN}}} = 2.76$ TeV.

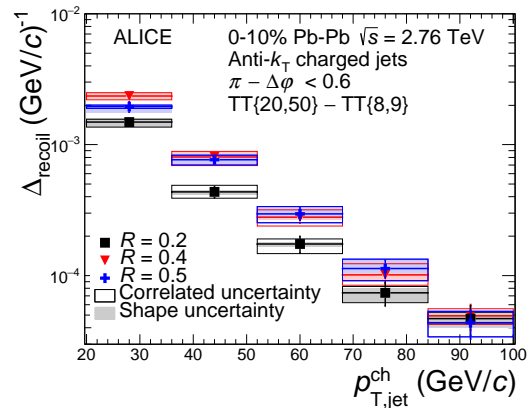


Figure 7. Fully corrected Δ_{recoil} distributions measured for 0–10% central Pb–Pb collisions at $\sqrt{s_{\text{NN}}} = 2.76$ TeV for anti- k_T jets with $R = 0.2, 0.4$ and 0.5 . The boxes indicate correlated and shape systematic uncertainties, see [29] for more details.

The requirement to have a high- p_T trigger in event introduces also some interesting biases on the selected sample of events and recoil jets. E.g., the parton that produces the trigger particle is more biased to be close to the surface of the collision zone [30], therefore the recoiling jet will have on average longer path length through the medium. Events containing a hard particle are also more biased to have larger number of participants or in other words to be more central. In both TT bins that are used this bias is the same.

In Figure 7, we present Δ_{recoil} distributions for several values of resolution parameter. The distributions are corrected for background fluctuations and detector effects. The medium-induced modification of jet fragmentation can be then searched for by means of the ratio

$$\Delta I_{AA} = \frac{\Delta_{\text{recoil}}^{\text{PbPb}}}{\Delta_{\text{recoil}}^{\text{pp}}} \quad (3)$$

where the Δ_{recoil} distribution measured in Pb–Pb is divided by the reference Δ_{recoil} distribution from pp collisions at the same center of mass energy per nucleon-nucleon pair. As ALICE data from pp at $\sqrt{s} = 2.76$ TeV have poor statistics we use a reference spectrum generated by the PYTHIA Perugia 2010 tune [10]. To test the reliability of the PYTHIA prediction, we have cross-checked the PYTHIA calculation with the measured Δ_{recoil} spectrum obtained from pp at $\sqrt{s} = 7$ TeV data, see Fig. 8. The pp analysis closely followed what was done for Pb–Pb. In general we can say that PYTHIA Perugia tunes provide predictions that are compatible with the measured data within the quoted statistical and systematic uncertainties.

Figure 9 shows the ΔI_{AA} obtained with PYTHIA Perugia 10 reference for anti- k_T jets with $R = 0.5$. The ratio exhibits a deficit in the yield of recoil jets. The magnitude of this suppression for jets with $R = 0.2$ and 0.4 is similar.

The Δ_{recoil} observable allows also to look for possible medium-induced modification of the jet shape. Figure 10 presents the ratio of Δ_{recoil} spectra of jets obtained for different R . The measured data are compared with vacuum pp trend predicted by PYTHIA. Within the quoted errors there is no evidence for significant energy redistribution w.r.t. PYTHIA pp data. This also means that there is no evidence for intra-jet broadening up to $R = 0.5$.

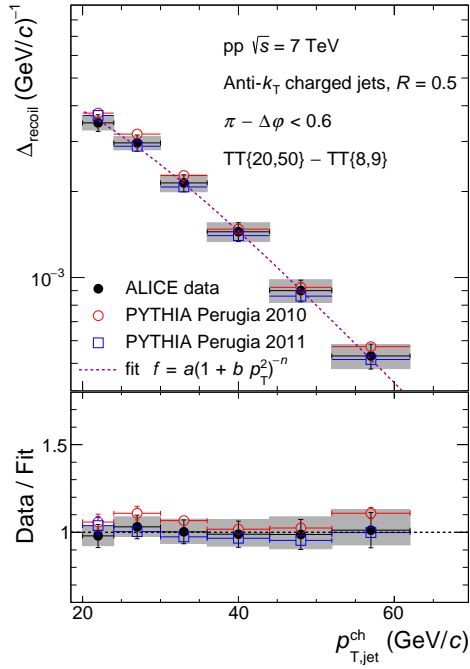


Figure 8. Upper panel: Δ_{recoil} distributions corresponding to anti- k_T jets with $R = 0.5$ in pp collisions at $\sqrt{s} = 7$ TeV. Comparison of measured data and PYTHIA Perugia 2010 and 2011 calculation. Systematic uncertainties on the measured data points are shown as gray boxes. The measured data are fit with a smooth function. Bottom panel: ratios of the data sets to the fit.

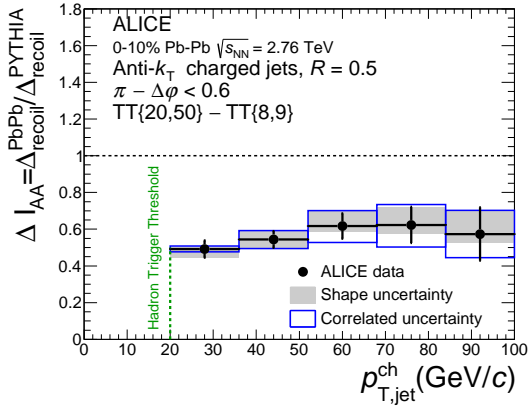


Figure 9. ΔI_{AA} , the ratio of Δ_{recoil} measured in central Pb-Pb and pp collisions at $\sqrt{s_{NN}} = 2.76$ TeV. Δ_{recoil} for pp collision was calculated with PYTHIA Perugia 10. The data corresponds to charged anti- k_T jets with $R = 0.5$.

6. Summary

Jets as well as other hard probes bring us information about the early states of matter produced in a collision of two nuclei. The picture of jet-medium interaction would, however, be incomplete

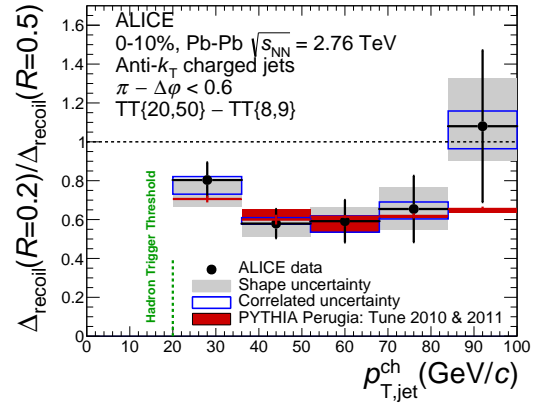


Figure 10. Ratio of Δ_{recoil} distributions corresponding to charged anti- k_T jets with $R = 0.5$ and $R = 0.2$. The black circles show the data measured in central Pb-Pb at $\sqrt{s_{NN}} = 2.76$ TeV. An estimate of the ratio in pp was obtained using PYTHIA Perugia tunes and is represented by the red bend. The width of the red bend is given by the difference between the Perugia 2010 and 2011 tune.

without the precise understanding of jet production and properties in elementary reactions such as pp. The measurement of particle type dependent jet fragmentation by ALICE in pp collisions at $\sqrt{s} = 7$ TeV thus helps to constraint available fragmentation models and event generators that are on the market.

Complex final state interaction gives rise to the baryon anomaly which is observed both in Pb–Pb and p–Pb systems at LHC energies. Measurements of Λ/K_S^0 ratio done with inclusive particles and jet fragments indicate that fragmentation of partons producing charged jets with $p_{T,\text{jet}}^{\text{ch}} > 20$ GeV/c is not a relevant source for the observed anomaly which thus seems to emerge from processes where the transferred Q^2 was lower.

Hadron-jet correlation measurements offer a new variety of observables well suited to study also low- p_T jets with large resolution parameter without inducing a fragmentation bias. PYTHIA Perugia tunes seem to provide reliable prediction for the measured h-jet observables in pp collisions, such as Δ_{recoil} . In Pb–Pb system, we see a suppression of the recoil jet yield but without a sign of intra-jet broadening for charged anti- k_T jets up to resolution parameter $R = 0.5$.

Acknowledgments

The work has been supported by the MEYS grant CZ.1.07/2.3.00/20.0207 of the European Social Fund (ESF) in the Czech Republic: Education for Competitiveness Operational Programme (ECOP) and by the grant LG 13031 of the Ministry of Education of the Czech Republic.

References

- [1] Salam G 2010 *Eur. Phys. J. C* **67** 637
- [2] Aad G *et al.* (ATLAS collaboration) 2010 *Phys. Rev. Lett.* **105** 252303
- [3] Chatrchyan S *et al.* (CMS collaboration) 2011 *Phys. Rev. C* **84** 024906
- [4] Aamodt K *et al.* (ALICE collaboration) 2008 *J. Instrum.* **3** S08002
- [5] Cacciari M, Salam G P and Soyez G 2012 *Eur. Phys. J. C* **72** 1896
- [6] Cacciari M and Salam G P 2008 *Phys. Lett. B* **659** 119
- [7] Höcker A and Kartvelishvili V 1996 *Nucl. Instrum. Meth. A* **372** 469
- [8] D’Agostini G 1995 *Nucl. Instrum. Meth. A* **362** 487
- [9] Adye T *CERN-2011-006* 313
- [10] Skands P 2010 *Phys. Rev. D* **82** 074018
- [11] Abelev B *et al.* (ALICE collaboration) 2014 nucl-ex/1411.4969
- [12] Lu X *et al.* (ALICE collaboration) 2014 *Nucl. Phys. A* **931** 428-432
- [13] Lu X *CERN-THESIS-2013-179*
- [14] Hess B *et al.* (ALICE collaboration) 2014 hep-ex/1408.5723
- [15] Adler S S *et al.* (PHENIX collaboration) 2003 *Phys. Rev. Lett.* **91** 172301
- [16] Adams J *et al.* (STAR collaboration) 2012 *Phys. Rev. Lett.* **108** 072301
- [17] Abelev B *et al.* (ALICE collaboration) 2013 *Phys. Rev. Lett.* **111** 222301
- [18] Song H and Heinz U W 2008 *Phys. Lett. B* **658** 279
- [19] Song H and Heinz U W 2008 *Phys. Rev. C* **77** 064901
- [20] Song H and Heinz U W 2008 *Phys. Rev. C* **78** 024902
- [21] Cuautle E, Jimenez R, Maldonado I, Ortiz A, Paic G and Perez E 2014 hep-ph/1404.2372
- [22] Topor Pop V, Gyulassy M, Barrette J and Gale C 2011 *Phys. Rev. C* **84** 044909
- [23] Brodsky S J and Sickles A 2008 *Phys. Lett. B* **668** 111-115
- [24] Werner K 2012 *Phys. Rev. Lett.* **109** 102301
- [25] Abelev B *et al.* (ALICE collaboration) 2014 *Phys. Lett. B* **728** 25
- [26] Ortiz A, Christiansen P, Cuautle E, Maldonado I and Paic G 2012 *Phys. Rev. Lett.* **111** 042001
- [27] Veldhoen M (ALICE collaboration) 2013 *Nucl. Phys. A* **910-911** 306-309
- [28] de Barros G O V *et al.* 2012 hep-ex/1208.1518
- [29] Abelev B *et al.* (ALICE collaboration) 2015 hep-ex/1506.03984
- [30] Renk T 2013 *Phys. Rev. C* **87** 2